Toxicon 129 (2017) 123–133

Contents lists available at ScienceDirect

Toxicon

journal homepage: www.elsevier.com/locate/toxicon

Parotoid, radial, and tibial macroglands of the frog *Odontophrynus cultripes*: Differences and similarities with toads

Pedro L. Mailho-Fontana [a], Marta Maria Antoniazzi [a], Isabela Rodrigues [a], Juliana M. Sciani [b], Daniel Carvalho Pimenta [b], Edmund D. Brodie Jr. [c, *], Miguel Trefaut Rodrigues [d], Carlos Jared [a]

[a] Laboratory of Cell Biology, Instituto Butantan, São Paulo, Brazil
[b] Laboratory of Biochemistry and Biophysics, Instituto Butantan, São Paulo, Brazil
[c] Department of Biology, Utah State University, Logan, UT, USA
[d] Department of Zoology, Universidade de São Paulo, São Paulo, Brazil

ARTICLE INFO

Article history:
Received 10 February 2017
Received in revised form
16 February 2017
Accepted 20 February 2017
Available online 21 February 2017

Keywords:
Amphibia
Odontophrynidae
Frog
Skin gland
Poison
Rhinella

ABSTRACT

Anuran integument is characterized by the presence of glands, some of which are responsible for toxin production. In some species these glands accumulate in parts of the body strategically located against predators, forming structures known as macroglands. This is the case for parotoid macroglands, on the dorsum of the head, tibial macroglands, on the rear limbs, and radial macroglands, on the forelimbs of toads and some other anurans. The toad *Rhinella jimi*, for example, simultaneously displays all three types of macroglands, which is unusual even among bufonids. Interestingly, considering the phylogenetic distance, the frog *Odontophrynus cultripes* (Odontophrynidae) also presents these three macroglandular types. In this study we analyze the morphology of *O. cultripes* macroglands and the chemical composition of their poison using an interdisciplinary approach. In this species, the parotoid, tibial, and radial macroglands consist of aggregates of elongated and juxtaposed poison glands, arranged in a honeycomb style, very similar to that of toads. Comparative analysis of these three macrogland types shows significant differences in both the morphology of secretory granules and biochemical composition. The present work on *O. cultripes* contributes to the evidence that amphibians, or at least anurans, share a basic design for all cutaneous glandular accumulations. The determinant factor for macroglandular formation may be the selective pressure for defense against predators.

1. Introduction

One of the striking features of amphibians is the presence of glands distributed throughout the skin. These glands are of two general types: mucous glands, mainly related to gas exchange and water balance, and granular (or poison) glands, related to chemical defense against predators and microorganisms (Toledo and Jared, 1995; Jared et al., 2015; Lutz, 1971). In many anurans and salamanders some granular glands are enlarged and aggregated forming glandular accumulations (macroglands) (Toledo and Jared, 1995; Duellman and Trueb, 1996). Macroglands may be located dorsally in the post-orbital region, termed parotoid macroglands (Wilber and Carroll, 1940; Tronchet, 1952; Lutz, 197; Toledo and Jared, 1995), and on the front and hind legs, termed radial and tibial (or paracnemic) macroglands, respectively (Toledo and Villa, 1987; Toledo and Jared, 1995; Jared et al., 2009). They are directly associated with chemical defense as their strategic positions are easily accessible to attack by a would-be predator (Brodie, 1983; Toledo and Jared, 1995; Antoniazzi et al., 2013; Mailho-Fontana et al., 2014a; Jared et al., 2014). The defensive mechanisms of these amphibians are considered “passive” because the predator itself triggers the expulsion of the poison when the macrogland is compressed by a bite (Jared et al., 2009; Mailho-Fontana et al., 2014a). The strategic location of the parotoids appears to play a major role in passive defense, and parotoids are the only type of macrogland present in most bufonids. Some bufonid species also have tibial glands, and a few, such as *Rhinella jimi* and *Incilius alvarius* possess all three types of macroglands.

Secretion from macroglands (and from glands scattered

* Corresponding author.
E-mail address: e.brodie@usu.edu (E.D. Brodie).

http://dx.doi.org/10.1016/j.toxicon.2017.02.022
0041-0101/

throughout the skin) can be very toxic to potential predators (Lutz, 1966; Brodie and Gibson, 1969; Barthalmus, 1989; Toledo and Jared, 1989, 1995; Clark, 1997). In bufonids, this secretion is composed primarily of steroids such as bufogenins and bufotoxins (Meyer and Linde, 1971; Habermehl, 1981). When in contact with the oral mucosa of many vertebrates, especially snakes, this secretion causes cardiac effects, increasing the contractile force of the heart (Licht and Low, 1968; Meyer and Linde, 1971; Habermehl, 1981; Sakate and Lucas De Oliveira, 2000). In frogs of the families Hylidae and Leptodactylidae the poison glands secrete mainly proteins and peptides with other pharmacological actions (Erspamer et al., 1986; Pukala et al., 2006; Siano et al., 2014).

Some frogs of the genus *Odontophrynus* (Odontophrynidae) have parotoid macroglands (Savage and Cei, 1965; Caramaschi and Napoli, 2012). *Odontophrynus cultripes*, in addition to having well-developed parotoids, is notable for also having radial and tibial macroglands. This diversity of macroglands in *O. cultripes* may be unique in non-bufonids. The three types of macroglands in *O. cultripes* secrete a variety of yet unknown and possibly bioactive substances with features distinct from bufonid secretions.

We aim to morphologically and biochemically characterize the macroglands of *O. cultripes* and compare them to those of bufonids. Our results suggest that *O. cultripes* macroglands are much less complex, lacking the apparatus that in some bufonids enables poison release through jets. We also speculate about the evolutionary development of macroglands in anurans.

2. Materials and methods

2.1. Animals

Odontophrynus cultripes Reinhardt and Lütken 1862 is a dark brown medium-sized frog with granular integument characterized by the presence of conspicuous ovoid parotoid macroglands and smaller but still stout forearm (radial) and tibial macroglands, along with other smaller glands. Males are smaller than females (SVL 60 vs. 70 mm) and generally remain buried most of the year, emerging only during the rainy season to breed. During the breeding season, males call for females from the border of permanent ponds, either exposed or concealed in soil depressions or leaf litter (Canelas and Bertoluci, 2007). In addition to protective coloration and the presence of large and highly conspicuous parotoid macroglands, *O. cultripes* exhibits both thanatosis and deimatic behaviors as complementary antipredator mechanisms (Hödl and Amézquita, 2001; Borges-Nojosa et al., 2016).

Odontophrynus cultripes occurs in the Brazilian states of Minas Gerais, São Paulo, and Goiás, usually above 800 m elevation (Caramaschi and Napoli, 2012) in both forested habitats and more open savannah-like shrub lands. Specimens were obtained in a banana grove at 890 m elevation near the border of a gallery forest at Serra dos Alves (−43.44298739, −19.49319332), state of Minas Gerais, Brazil under collecting permits ICMBIO (SISBIO #23202-1 and #10126-1).

All aspects of the study were carried out in accordance with protocols approved by the Ethics Committee on Animal Use of Instituto Butantan (protocol #3539021015).

2.2. Experimental design

Four specimens of *Odontophrynus cultripes* had right parotoid, tibial and radial macroglands manually compressed for secretion collection. Immediately after compression, the animals were euthanized with thiopental (50 mg/kg). Compressed and uncompressed macroglands were dissected and processed for morphological study. For biochemical characterization, a pool of secretion from all four specimens was extracted from each type of macrogland. The secretion samples were diluted in ultrapure water containing 0.1% trifluoroacetic acid (TFA) and 5% acetonitrile (ACN).

2.3. Histology

Samples of integument from the dorsum and venter and entire parotoid, radial, and tibial macroglands were prepared for light microscopy. Each macrogland was transversely cut into four pieces and fixed together with integument samples in 4% formaldehyde (made from paraformaldehyde) buffered in 0.1 M phosphate buffer, pH 7.2 (Junqueira, 1995) for 48 h. One piece of each macrogland was embedded in glycol metachrylate (Leica historesin), sectioned 0.5–4 μm thick, and stained with toluidine blue-fuchsin (Junqueira, 1995). Other pieces of each macrogland were embedded in paraffin, both in transverse and longitudinal orientations; sections 4–6 μm thick were stained with picrosirius red and examined using light microscopy using polarized light for identification of collagen fibers (Junqueira et al., 1979). Glycol metachrylate sections also were stained using bromophenol blue, periodic acid-Schiff (PAS) combined with alcian blue at pH 2.5, and the Masson-Fontana, and von Kossa methods (Bancroft and Steven, 1990) for detection of proteins, neutral and acid mucosubstances, biogenic amines (or alkaloids), and calcium, respectively. Light micrographs were taken with an Olympus BX51 light microscope equipped with a digital camera and Image-Pro Express software (Media Cybernetics).

2.4. Unidimensional electrophoresis (SDS-PAGE)

To determine the molecular weight of the protein content of skin secretions, 15 μg of each sample were analyzed by 12% sodium dodecyl sulfate polyacrylamide gel electrophoresis (SDS-PAGE), under reducing conditions, according to the method described by Laemmli (1970). Gels were stained by silver nitrate.

2.5. Chromatography (RP-HPLC) and mass spectrometry

Secretion samples were analyzed by reversed phase high performance liquid chromatography (RP-HPLC) using a binary HPLC system (20A Prominence, Shimadzu Co., Japan) with mass spectrometry (ESI-IT-ToF, Shimadzu Co., Japan). The samples were loaded in a C18 column (ACE C18, 5 μm, 100 Å, 50 mm × 2.1 mm) in a two-solvent system: (A) acetic acid/H_2O (1:1000) and (B) acetic acid/acetonitrile/H_2O (1:900:100). The content was eluted at a constant flow rate of 0.2 mL min^{-1} with a 0–100% gradient of solvent B over 15 min, after a 5 min isocratic elution with 0% B. The HPLC column eluates were monitored by a Shimadzu SPD-M20A PDA detector, scanning from 200 to 500 nm (1 nm steps), and mass spectrometry.

For mass spectrometry analysis, samples from RP-HPLC were ionized by ESI in positive mode. The interface voltage was kept at 4.5 kV, the detector voltage was 1.76 kV, and the capillary temperature was 200 °C. Instrument control and data acquisition were conducted by LCSolutions (Shimadzu Co., Japan), and the mass spectra were collected in a range of 50–2000 m/z. For the MS/MS analysis, argon collision energy was kept at 50% and precursor ions were selected under a 0.5 m/z window. Peaks and ions were identified in accordance with their physicochemical characteristics and by comparing the previously reported fragmentation pattern spectra (McClean et al., 2002; Maciel et al., 2003; Daly et al., 2005; Ye and Guo, 2005; Liu et al., 2010; Sciani et al., 2013).

3. Results

3.1. Anatomy of the integument and macroglands

The integument of *Odontophrynus cultripes* (Fig. 1A), especially in the dorsal region, is very rough and covered with tubercles of different sizes. Some of these tubercles are very enlarged, forming glandular clusters that anatomically correspond to the parotoid, radial, and tibial macroglands of the toad *Rhinella jimi* (Jared et al., 2009) (Fig. 1C). In *O. cultripes*, however, the parotoids and the dorsal tubercles stand out from the rest of the body because of their contrasting coloration, ranging from brown-orange to red, surrounded by a dark halo. Because of the apparent anatomical equivalence of *O. cultripes* macroglands to those of toads, we will refer to them by the same designations: "parotoid," "tibial," and "radial".

In *O. cultripes,* each parotoid is always accompanied by two or three smaller glandular accumulations (ancillary macroglands), forming a characteristic macroglandular complex (Fig. 1A). The parotoid is always reniform, different from the ancillary macroglands that are quite variable in shape. A common feature of the ancillary macroglands is the presence of fusion bridges among them that, in some cases, transform them into one single structure distinct from the parotoid.

The tibial and radial macroglands of *O. cultripes* are less prominent than parotoid macroglands and spread over a large part of the limb surface, distinctive more for the area they occupy than for their volume. Unlike parotoids, the tibial and radial macroglands always appear as a single structure and seem not to form macroglandular complexes. However, like the parotoids, these structures are anatomically positioned in such a way that their surface is always exposed and within reach of the bite of an attacking predator.

All of these macroglands are composed of juxtaposed alveoli, each one bearing a secretory poison gland of large dimensions, and

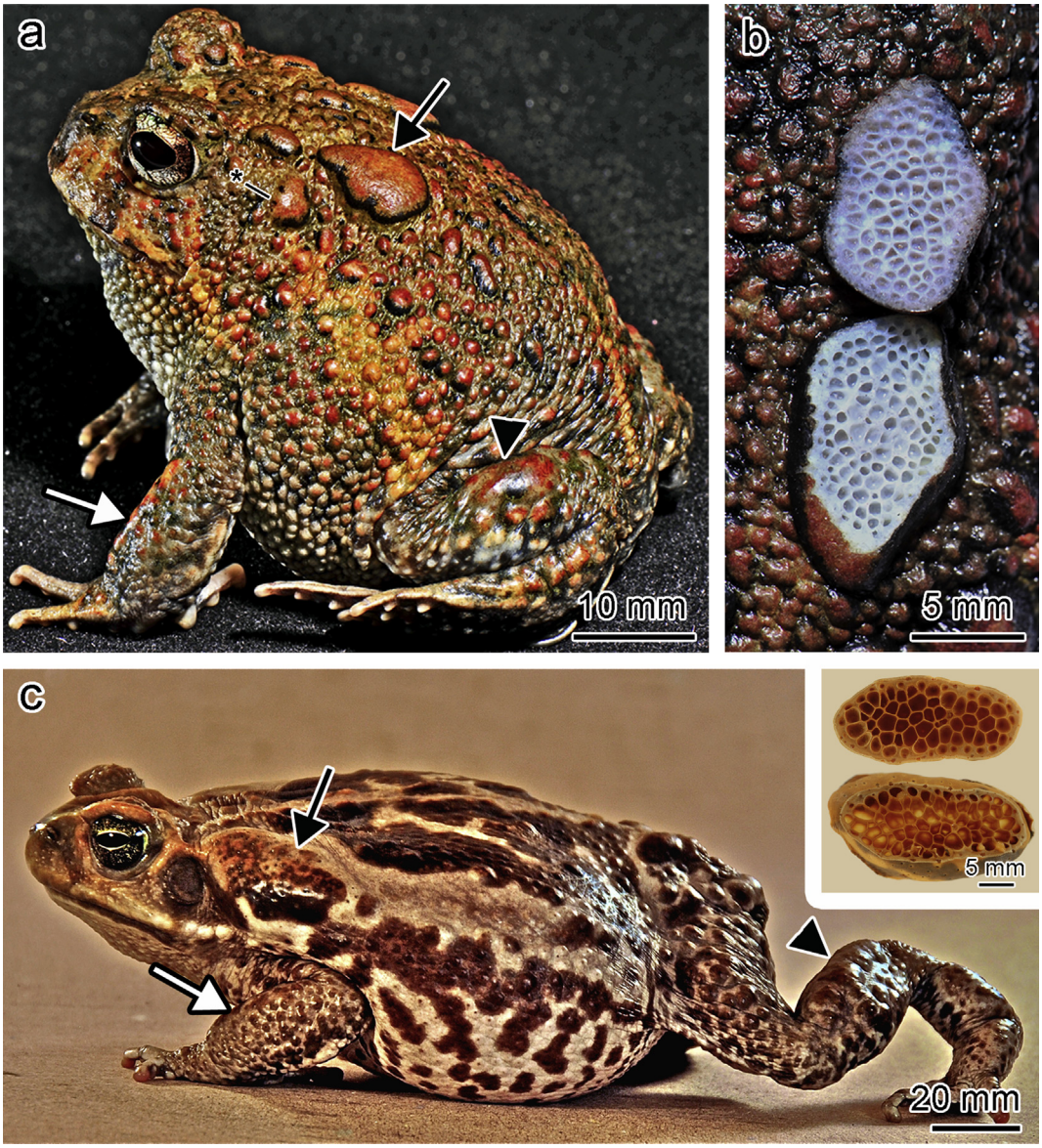

Fig. 1. Macroglands of *Odontophrynus cultripes*. (a) Lateral view of an adult frog showing parotoid (black arrow), ancillary (asterisks), radial (white arrow), and tibial (arrowhead) macrogland; (b) Parotoid of *O. cultripes* sectioned in horizontal plane showing the honeycomb-like arrangement in both superior and inferior portions observed in all macroglands; (c) The toad *Rhinella jimi* exhibiting the parotoid (black arrow), radial (white arrow), and tibial (arrowhead) macroglands. Note that anatomical position of macroglands is very similar to *O. cultripes*. The insert shows the similarity in the honeycomb-like arrangement of macroglands of both species.

the entire set constituting a single honeycomb-like structure (Fig. 1B). The alveoli located in the dermis are surrounded by dense collagen fibers that support the honeycomb-like architecture, which remains unchanged even after being compressed for poison expulsion.

3.2. Histology of the integument

As in other anurans, the entire integument of *O. cultripes* is characterized by the presence of two basic glandular types: the granular (or poison) glands and the mucous glands (Fig. 2A). In the dorsal integument, these two glandular types are larger and more numerous than in the ventral region and their distribution is always related to the presence of tubercles. The epidermis is composed of 5–6 cell layers, and the outermost layer, the stratum corneum, is quite developed (7.7 ± 0.5 μm thick). Immediately below the epidermis lies the dermis, composed of the spongious and compact layers, which follows the general pattern of vertebrates. Both

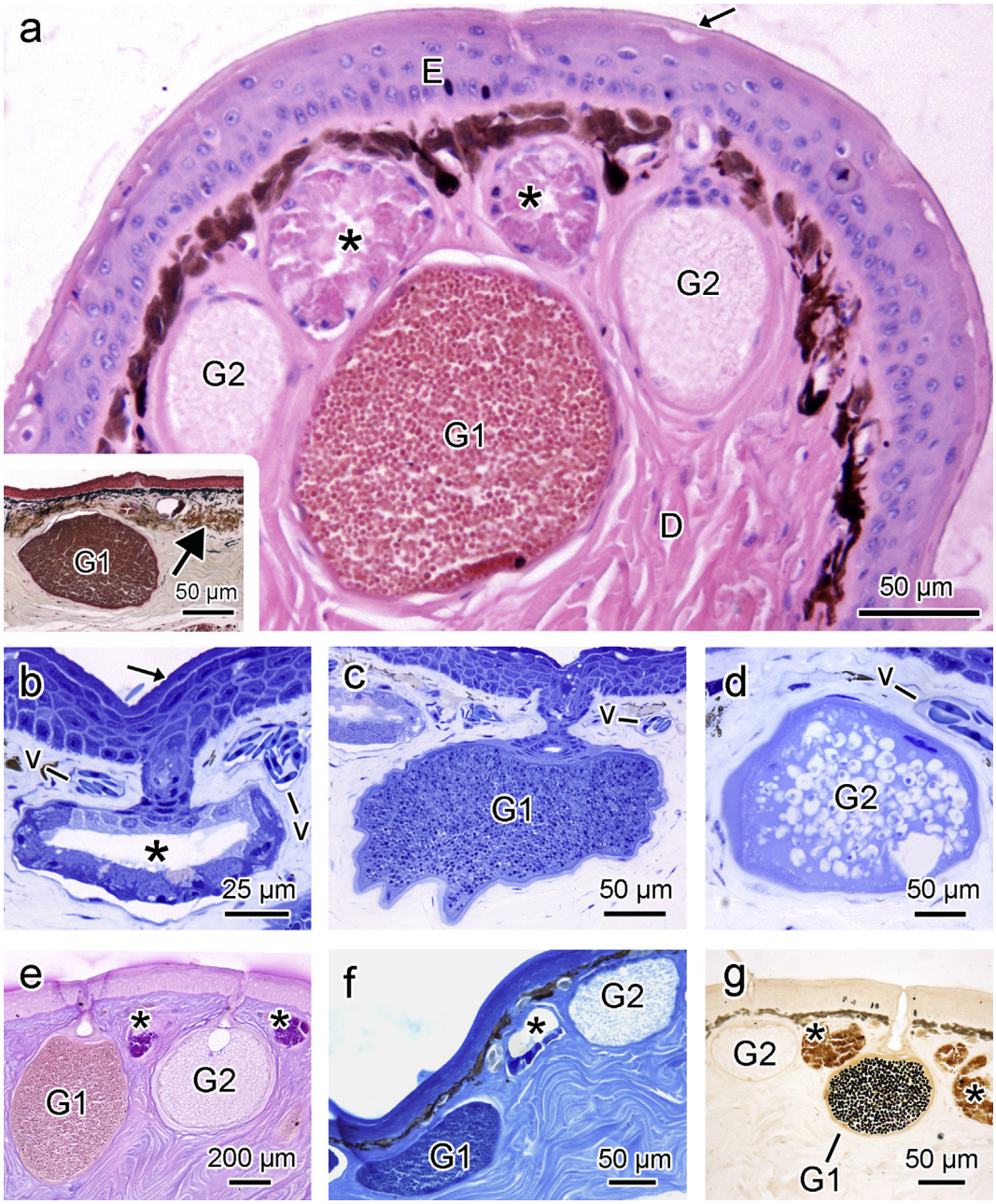

Fig. 2. Histology of the dorsal tubercles of *Odontophrynus cultripes*. (a) General view showing mucous glands (*) and two distinct types of granular poison glands (G1 and G2) in the dermis (D). The arrow points to the stratum corneum of the epidermis (E). Hematoxylin-eosin staining. The insert shows the calcified dermal layer (arrow). Von Kossa staining. (b) High magnification of a mucous gland (*). Blood vessels (V), Stratum corneum (arrow). Toluidine blue-fuchsin staining. (c) Type 1 granular gland (G1), which is found more frequently in dorsal skin. Blood vessel (V). Toluidine blue-fuchsin staining. (d) Type 2 granular gland (G2). Blood vessel (V). Toluidine blue-fuchsin staining. (e) PAS + alcian blue at pH 2.5. Most cells of the mucous glands (*) and the content of Type 1 granular glands (G1) are positive for neutral mucopolysaccharides, but none of the glands is positive for acid mucopolysaccharides. Type 2 granular glands (G2) are negative to both reactions. (f) Some cells of the mucous glands (*) and Type 1 granular gland (G1) are positive to protein (Bromophenol blue). Type 2 granular gland (G2) is negative. (g) Type 1 granular glands (G1) and mucous glands (*) are both positive to alkaloids (Modified Masson-Fontana); Type 2 granular glands (G2) are negative.

granular and mucous glands are embedded in the spongious layer, surrounded by connective tissue; the pigment layer is present beneath the epidermis together with an extensive network of blood vessels (Fig. 2A–D). The compact layer is mainly composed of collagen fibers with loose organization and is barely distinguishable from the spongious layer (Fig. 2A–D). The subcutaneous tissue, the innermost layer of the integument, shows nerves and an extensive network of large-caliber blood vessels.

The spongy layer of the dermis is partially occupied by a discontinuous and dispersed calcified layer, located just beneath the pigment cells (Fig. 2A, insert). All glandular types are connected to the surface through ducts and are wrapped in a monolayer of myoepithelial cells (Fig. 2A–D). In the granular glands, the duct has an internal canal that, in its inner extremity, is connected to a blind vestibule separating the duct from the poison inside the gland (Fig 2C, E–G).

Based on morphological and histochemical characters, two types of granular glands were identified in *O. cultripes*, here named Type 1 and Type 2 (Fig. 2A). Both types are distributed throughout the integument, are wrapped by a monolayer of myoepithelial cells, and contain spherical granules embedded in a cytoplasmic matrix (Fig. 2A–D). The granules fill the glands including the peripheral region where the syncytial nuclei are located. The granules at the periphery, especially the smaller (and probably more immature), are denser.

The Type 1 granular glands are more common and measure 180 ± 49.45 μm tall and 162 ± 7.63 (se) μm wide. Presence of neutral mucopolysaccharides, proteins, and biogenic amines were indicated by reaction to histochemistry. When stained with toluidine blue-fuchsin; the granules show a characteristic heterogeneity, varying from quite light to dark blue (Fig. 2C). The secretion granules of these glands are positive for PAS, bromophenol blue, and Masson-Fontana (Fig. 2E–G), indicating the presence of neutral mucopolysaccharides, proteins, and biogenic amines, respectively. Type 2 glands are smaller and measure 105.68 ± 49.45 μm tall and 83.08 ± 38.01 μm wide. They have a well-developed cytoplasm (Fig. 2D) with smaller granules that, unlike Type 1 granules, do not react to the above histochemical methods (Fig. 2D–G).

The rounded mucous glands constitute acini, which are formed by a peripheral monolayer of cells with basal nuclei and a central lumen (Fig. 2A–B). These glands are 77.5 ± 9.91 μm tall and 61.83 ± 8.47 μm wide and its cells are positive for neutral mucopolysaccharides, proteins and biogenic amines.

3.3. Histology of the macroglands

In *Odontophrynus cultripes*, parotoid, tibial, and radial macroglands are characterized by large dorsal accumulations of elongated glands, individually housed in alveoli, occupying practically the entire height of the dermis, which is about six times thicker than the rest of the dorsal dermis (Fig. 3A). In addition to the elongated glands, in all three types of macroglands the regular, smaller granular glands (both Type 1 and Type 2) and mucous glands are also present in the upper stratum of the dermis that is juxtaposed to the epidermis (Fig. 3A). In transverse sections the glandular alveoli assume the shape of small, juxtaposed bottles. The central alveoli are larger, decreasing in size towards the periphery, which confers a domed shape to the macrogland (Fig. 3B). In the parotoids, the most protuberant macroglands, central alveoli average 1835.43 ± 70.39 μm tall and 615.73 ± 46.39 μm wide. The tibial macroglands are of medium size, averaging 711.37 ± 54.68 μm high and 522.94 ± 112.16 μm wide. Finally, in the radial macroglands, the least protuberant ones, the alveoli average 445.77 ± 80.02 μm tall and 246.07 ± 27.85 μm wide. As in the body skin, the calcified layer is diffuse and discontinuous in all three types of macroglands, occupying the uppermost portion of the dermis above the alveoli (Fig. 3A insert). In the radial macroglands, the calcified layer seems generally more developed than in the other two types of macroglands.

The glandular alveoli are surrounded by dermal connective tissue, rich in blood vessels. Analysis under polarized light of sections stained with picrosirius red shows that the connective tissue supporting the alveoli is primarily composed of Type-I collagen fibers, stained red (Fig. 3B).

The general morphology of the glands inside the macroglandular alveoli is quite similar to that of common skin granular glands: they are surrounded by a unicellular myoepithelial layer and are formed by a syncytium filled with secretory granules (Fig. 3C–E). These granules are positive for neutral mucopolysaccharides, proteins, and biogenic amines much like those of the Type 1 granular glands predominant in the skin of the entire body.

However, with respect to morphology, these poison granules have peculiarities that distinguish the parotoid from the tibial and radial macroglands. In the parotoid macroglands, the granules vary in size and are heterogeneously dispersed throughout the cytoplasm. Compared to the tibial and radial macroglands, the poison granules of the parotoids are surrounded by a more developed cytoplasm and are more intensely stained with toluidine blue (Fig. 3C–E). In the radial macroglands, the granules are smaller and quite heterogeneous in relation to toluidine blue staining, similarly to the granules of Type 1 skin glands. The three types of macroglands of *O. cultripes* differ markedly in both structure and histochemistry (Table 1).

Each macroglandular secretory alveolus is connected to the outside through a duct that releases the secretion. The duct is partially obstructed in its innermost portion by epithelial tissue (Fig. 4A). When macroglands were manually compressed, the secretion was released as drops on the skin, not as jets as in toads. Immediately after compression, many alveoli showed emptied syncytia, with little secretion inside (Fig. 4B, C). Comparing compressed and uncompressed macroglands reveals no significant architectural changes in organization of collagen fibers surrounding the alveoli (Fig. 4D). Furthermore, among these fibers, blood vessels that irrigate the dermis around the alveoli are frequently seen without ruptures (Fig. 4B insert).

3.4. Biochemical characterization of the macroglands secretions

The secretions of parotoid and tibial macroglands have very similar SDS-PAGE profiles, composed of bands of high, medium, and low molecular mass. The largest diversity of proteins is in the central region of the gel, between 66 kDa and 30 kDa. The secretion of the radial macrogland has distinctly different low quantity and diversity of proteins (Fig. 5).

The secretion of the radial macrogland also shows a distinctive chromatographic profile, differing from that of parotoid and tibial macroglands (Fig. 6). The secretions of the three types of macroglands are categorized as alkaloids, steroids, and peptides (Tables S1, 2). There are marked differences among secretions from the three types of macroglands in the diversity and amount of compounds within each of these chemical groups. Parotoid and tibial macroglands had the richest secretions in terms of number of peptides. Moreover, the variety of compounds with low molecular mass such as alkaloids and steroids is greater in the radial secretion. Only 5.9% of the compounds are common to all three types of macroglands. In contrast, the sum of the exclusive compounds totals about 73% (21% only in the tibial, 25% only in the parotoid, and 27% only in the radial macroglands) (Fig. 6; Table 2). An additional 10% are found in both parotoid and tibial macroglands; 5% in both parotoid and radial macroglands; and 5% in both tibial and radial macroglands.

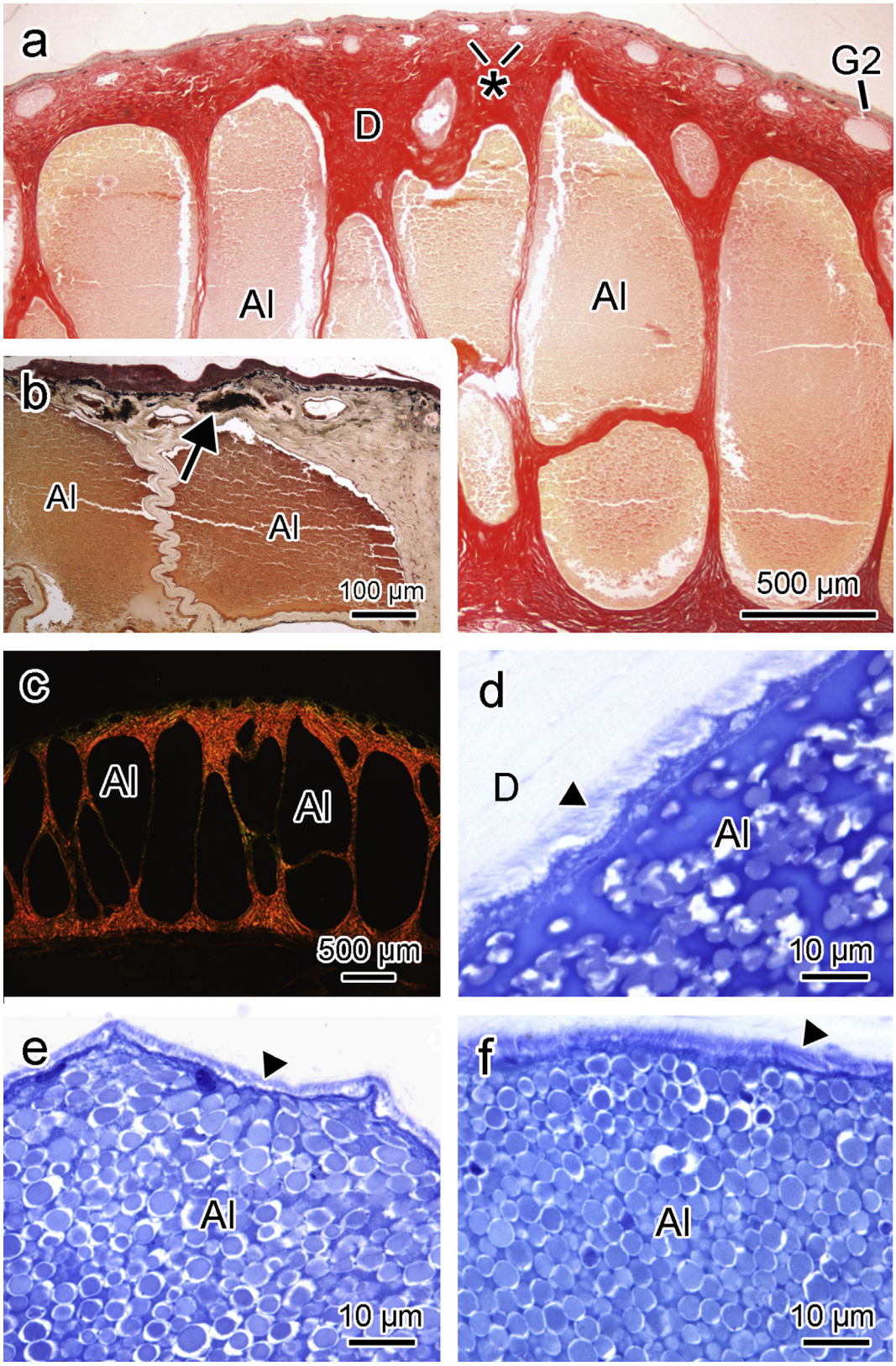

Fig. 3. Histology of the macroglands of *Odontophrynus cultripes*. (a) Transverse histological section of the parotoid macrogland showing the accumulation of large and elongated alveoli (Al), which make this region much thicker than the rest of the skin. Dermis (D), Mucous glands (*), Type 2 granular glands (G2), Picrosirius red staining examined under polarized light microscopy. (b) Discontinuous calcified dermal layer (arrow) in the tibial macrogland, located above the alveoli. Von Kossa histochemical method. (c) Polarized light microscopy of the parotoid highlighting the alveoli (Al) framework, constituted of dermal connective tissue mainly composed of collagen Type-I fibers (reddish color). Picrosirius staining. (d, e, and f) High magnification of part of an alveolus (Al) of the parotoid (d), tibial (e), and radial (f) macroglands. Note the difference in the morphology of the glandular content (granules) in the three types of macroglands. Myoepithelial layer (arrowhead). Dermis (D), Toluidine blue-fuchsin staining.

Table 1
Summary of the main features characterizing the different types of granular glands of *Odontophrynus cultripes*.

Granular gland	Toluidine blue-fuchsin	Size of granules (μm)	PAS	AB	BB	M-F
Type 1	Heterogeneously stained granules. Discrete syncytial cytoplasm.	3.54 ± 0.50 (2.57–4.33)	+	–	+	+
Type 2	Discrete granules. Well-developed syncytial cytoplasm.	3.23 ± 0.90 (2.95–4.60)	–	–	–	–
Radial	Few and heterogeneously stained granules. Discrete syncytial cytoplasm.	4.73 ± 0.64 (3.73–5.89)	+	–	+	+
Tibial	Homogeneously stained granules. Discrete syncytial cytoplasm.	4.87 ± 0.47 (4.14–5.87)	+	–	+	+
Parotoid	Homogeneously stained granules. Well-developed syncytial cytoplasm.	5.47 ± 0.61 (4.71–6.82)	+	–	+	+

PAS, Periodic Acid-Schiff; AB, Alcian Blue stain; BB, Bromophenol Blue stain; M-F, Masson-Fontana stain.

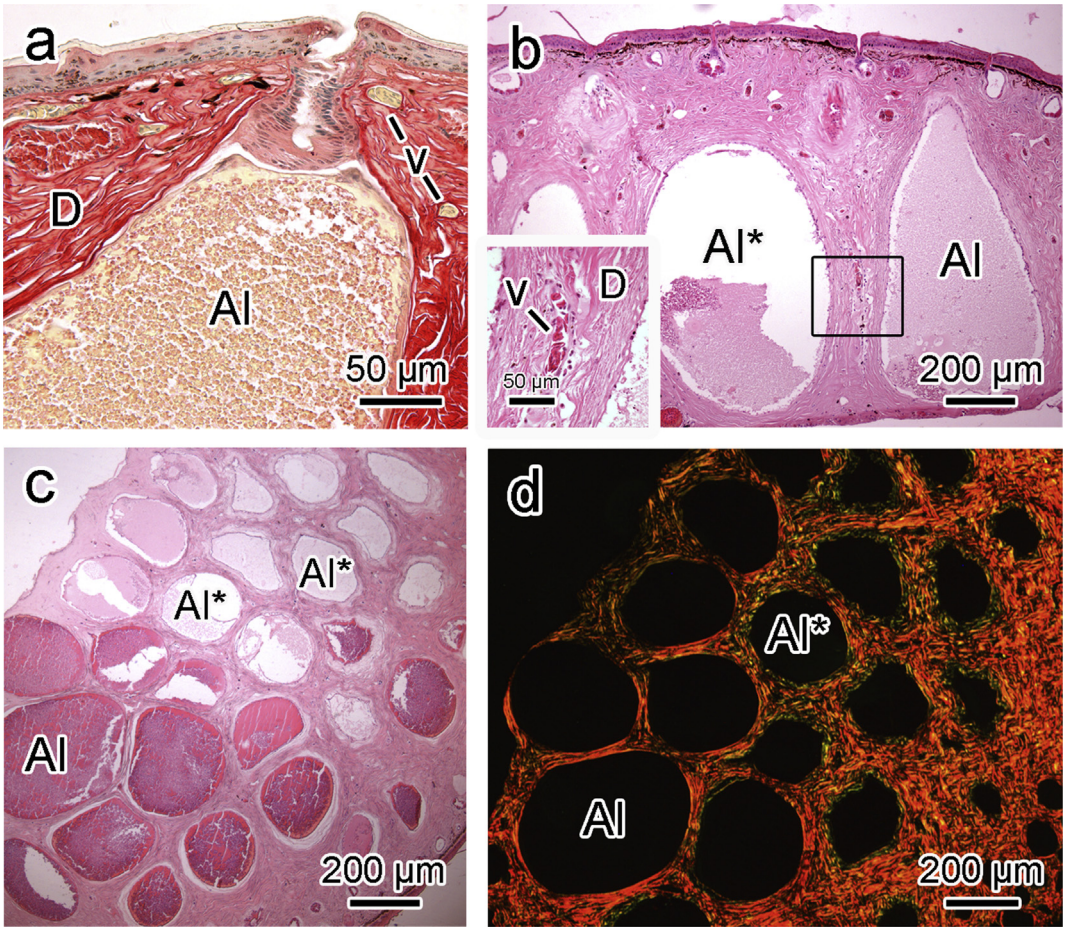

Fig. 4. Histology of the macroglands of *Odontophrynus cultripes* before and after manual compression. (a) Longitudinal section of the ductal region of parotoid alveoli (Al) before manual compression. Note the discrete lumen along the length of the duct and obstruction in the innermost portion. Dermis (D), Blood vessels (V). Picrosirius staining. (b) Manually compressed parotoid. Many alveoli are collapsed (Al*) while others are full of secretion (Al). Insert. Higher magnification of the selected area in the anterior image showing the blood vessels (V) in the dermis (D) between two alveoli affected by manual compression. Hematoxylin-eosin staining. (c) Longitudinal section of parotoid macrogland after manual compression. Note some alveoli full of secretion (Al) and others partially or completely empty (Al*). Hematoxylin-eosin staining. (d) Polarized light microscopy of the macrogland after manual compression. The arrangement of the collagen fibers in the dermis is not affected by compression and is similar to that observed in the intact macrogland. Alveoli (Al), Empty alveoli (Al*). Picrosirius staining.

The three macroglands of *Odontoprhynus cultripes* yield alkaloids and steroids known in other amphibians but with varying distributions in each of them. Among the alkaloids, dehydrobufothionine is present exclusively in the parotoid secretion and dehydrobufotenine is found only in the tibial secretion, while bufotenin is present in both parotoid and tibial secretions. Among steroids, resibufaginol is present in all three macroglands while resibufagine and desacetylcinobufotaline are found in the parotoid and radial macroglands.

Macrogland secretions have a low number of types of peptides. Parotoids have nine peptides, tibials have ten peptides, whereas radials have only one peptide. The parotoids share eight peptides with tibial macroglands and one with the radial macroglands. Thus, parotoids have one exclusive peptide and tibials have two. The single peptide in the radial macroglands was not exclusive. All these peptides are previously unknown amino-acid sequences and have no similarity to other known peptides (Table S1).

4. Discussion

Many types of cutaneous glandular accumulations related to defense have been identified in amphibians; toads (Almeida et al., 2007; Jared et al., 2009; Mailho-Fontana et al., 2014a), tree frogs (Antoniazzi et al., 2013), leiopelmatids (Melzer et al., 2011) and

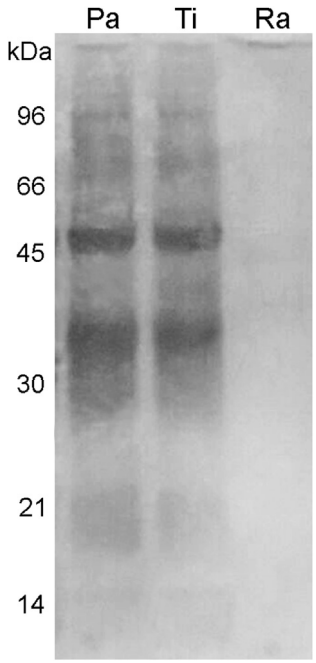

Fig. 5. SDS–PAGE of secretion extracted from the three types of macroglands of *Odontophrynus cultripes*. Parotoid (Pa), tibial (Ti), and radial (Ra) secretion. The numbers (kDa) at the left correspond to the molecular mass markers.

Toad (bufonid) parotoids are by far the most studied glandular accumulations in amphibians. From the end of the nineteenth century, works have described these structures only from the morphological point of view, without any integration of morphology with biology and natural history (Wilber and Carroll, 1940; Tronchet, 1952; Lutz, 1966; Hostetler and Cannon, 1974; Licht and Sever, 1993). However, more recent papers have examined skin glands in an interdisciplinary context, greatly increasing the understanding of general morphology, biochemistry, and functioning of glandular accumulations (Cannon and Palkuti, 1976; Daly et al., 2005; Antoniazzi et al., 2013; Mailho-Fontana et al., 2014a; Siano et al., 2014; Chammas et al., 2015).

Analysis of the distribution of integumentary granular glands in amphibians suggests the position of macroglands is related to defense against predators. These structures seem to have developed in locations easy accessible to the mouth of predators. In toads, the dorsal postorbital region and possibly, to a lesser extent, the outer surface of the front and rear legs are obviously exposed to attack.

Moreover, there is a close relationship between amphibian defensive behavior and the location of macroglands, resulting in predator attack directed specifically at the macroglandular regions (Jared et al., 2009; Brodie, 1983). For example, in general, when toads feel threatened, they inflate the lungs and take a stereotypical head-down posture presenting the parotoids to the would-be predator (Jared et al., 2009). When the frog *Eupemphix nattereri* (formerly *Physalaemus nattereri*) is threatened, it also assumes a

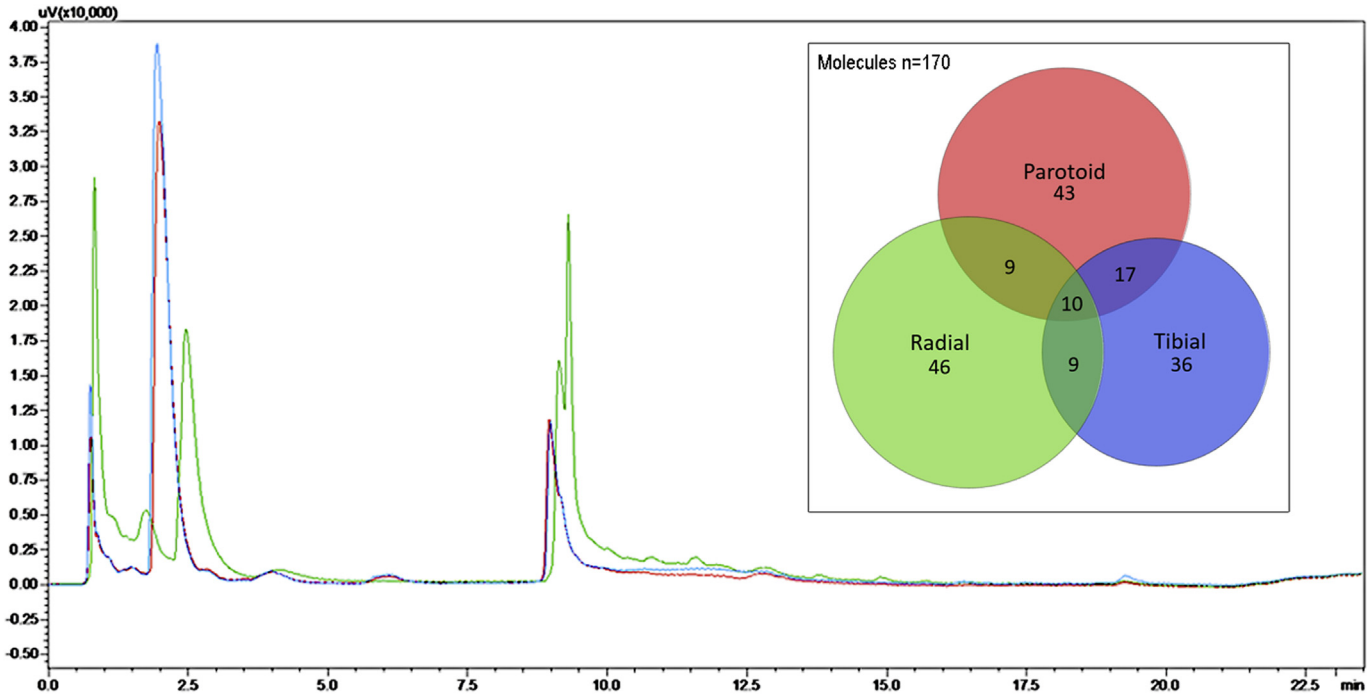

Fig. 6. C18-RP-HPLC of secretion extracted from the three types of macroglands of *Odontophrynus cultripes*. Parotoid (red), tibial (blue), and radial (green) chromatographic profiles. Circle intersection graph shows the sharing of molecules that were found by mass spectrometry. Note the major similarity between parotoid and tibial secretions.

salamanders (Brodie, 1983; Brodie and Smatresk, 1990; Licht and Sever, 1993) have parotoid macroglands that are positioned on the dorsal postorbital region (Toledo and Jared, 1995). In addition, tibial (or paracnemic) and radial macroglands may be located on the outer surface of the rear and front legs, respectively (Toledo and Villa, 1987; Toledo and Jared, 1995).

series of stereotypical body postures, inflating the lungs, turning back, extending the hind legs, and raising the lower back. In this posture, a prominent pair of round black inguinal macroglands is exposed, giving the impression of a face with two large eyes (Hödl and Amézquita, 2001; Lenzi-Mattos et al., 2005). If an attack occurs, the inguinal macroglands release a potent secretion repulsive to

Table 2
Distribution of compounds among parotoid, tibial, and radial macroglands of *Odontophrynus cultripes*.

Number of compounds in *Odontophrynus cultripes*			
170			
Parotoid		Tibial	Radial
Number of compounds per macrogland			
79		72	74
Number of exclusive compounds			
43		36	46
Parotoid/Radial/Tibia	Parotoid/Tibial	Parotoid/Radial	Tibial/Radial
Number of shared compounds			
9	17	9	9

predators.

One of the rare anuran species having parotoid, tibial, and radial macroglands is the toad *R. jimi*. There are no significant differences in the morphology and ultrastructure among the three types of macroglands present in *R. jimi* (Toledo and Villa, 1987; Jared et al., 2009; Mailho-Fontana et al., 2014b).

Odontophrynus cultripes, despite belonging to a family (*Odontophrynidae*) with a phylogenetic position distant from the bufonid *R. jimi*, has similar macroglands positioned in equivalent regions. The internal morphology of their macroglands basically follows the typical honeycomb-like design characteristic of the parotoids of toads (Jared et al., 2009) and tree frogs of the family Phyllomedusidae (Antoniazzi et al., 2013), and the inguinal macroglands of some frogs (Lenzi-Mattos et al., 2005).

However, unlike most toads, the coloration of the macroglands of *O. cultripes*, especially the parotoids, is distinctive from the rest of the body. The dark line skirting the base of the parotoids and ancillary and dorsal tubercles seems to highlight their presence, probably contributing to aposematism and thereby discouraging predator attack.

The genus *Odontophrynus* consists of 11 species distributed in three species groups, *O. americanus*, *O. occidentalis*, and *O. cultripes* (Caramaschi and Napoli, 2012). The presence of macroglands is one of the morphological characters used to distinguish the different species. Morphological analysis of the integument and its glands in these frogs indicates a tendency to form highly developed macroglands, particularly in the *O. cultripes* group. Unfortunately, data on the natural history of *Odontophrynus* are scarce.

The morphology of the three types of macroglands in *O. cultripes* always remains constant. In contrast, the small glandular accumulations (ancillary macroglands) surrounding the parotoid, although always present, show great variation in shape and size. Considering the great integumentary adaptability of amphibians in general, and the morphological and biochemical richness of their integumental glands specifically, it is suggestive that the origin of the parotoids has occurred due to the gradual fusion of these little glandular satellites in response to selective pressure imposed by defense against predators.

The morphology of the integument of *O. cultripes* follows the pattern present in most amphibians being well vascularized and rich in mucous and granular glands. Moreover, the presence of two types of granular glands (here named Type 1 and Type 2) with quite different morphological characteristics, is a common feature in many other frog species (Melzer et al., 2011; Delfino et al., 1990, 1998; Felsemburgh et al., 2007; Mailho-Fontana, 2012; Regueira et al., 2016). In such glands, the characteristic poison granules are always observed completely filling the interior of the glandular syncytium. An interesting fact, however, is that in *O. cultripes*, as well as in other anuran species we have studied (unpublished data), we have frequently observed a remarkable difference between the two glandular types concerning the histochemical properties of the poison granules. The morphological and histochemical peculiarities of these glands suggest that they may represent an amplification of the defensive repertoire of the frogs against predators and microorganisms.

Studies have shown that tissue regeneration and refilling of poisonous secretion in bufonids follow a clear sequence of cellular events (Jared et al., 2009, 2014). Toad parotoid granular glands have a system of functioning and poison refilling much more complex than those of phyllomedusids and *O. cultripes*. In toads, after poison expulsion from alveoli, the syncytia collapse at the alveolar center and alveoli are completely surrounded by loose connective tissue that expands centripetally from the alveolar walls (Jared et al., 2009, 2014). The ejection mechanism observed in toad parotoids is a consequence of the morphology of alveoli, which have ducts obstructed by an epithelial plug that acts like a cork capping a bottle (Jared et al., 2009, 2014; Antoniazzi et al., 2013; Mailho-Fontana et al., 2014a,b). When the pressure inside the alveoli becomes greater than that supported by the plug, this structure breaks up, propelling the poison jet to the outside (Jared et al., 2009, 2014; Antoniazzi et al., 2013; Mailho-Fontana et al., 2014a,b). In *O. cultripes* the thickening noted in the duct walls may have a role similar to that of the epithelial plug, albeit with much less efficiency. In *O. cultripes*, the loose connective tissue, does not seem to play any significant role in glandular physiology and syncytia collapse is not evident.

Additionally, in parotoids of toads, there are characteristic differentiated mucous glands distributed around the outer portion of each duct (Jared et al., 2009, 2014; Antoniazzi et al., 2013; Mailho-Fontana et al., 2014a,b). In macroglands of *O. cultripes*, as well as in parotoids of phyllomedusid tree frogs (Antoniazzi et al., 2013), such glands do not exist. Although the function of these differentiated mucous glands is not yet clear, it has been speculated that they might play a role in alveolar physiology, and their secretion could be part of the composition of the toad poison (Antoniazzi et al., 2013).

The diversity of compounds found among the three types of macroglands in *O. cultripes* contrasts with that observed in *R. jimi*, in which the composition is homogeneous in all macroglands (Mailho-Fontana et al., 2014b). Corroborating the histochemical results, biochemical data show that *O. cultripes* macroglands contain low molecular mass molecules such as steroids and alkaloids in addition to proteins and peptides. The low-mass components identified in the secretion of *O. cultripes*, especially the steroids, also are typically found in the poison of toads (Sciani et al., 2013; Mailho-Fontana et al., 2014a,b; Regueira et al., 2016). However, the presence of peptides is a common feature in secretions of tree frogs (hylids) (Toledo and Jared, 1995; Clark, 1997; Siano et al., 2014) and other frogs (leptodactylids) (Toledo and Jared, 1995; Rollins-Smith et al., 2005), but peptides are rarely found in toad

secretions (Rash et al., 2010). Thus, the composition of *O. cultripes* macrogland secretion has certain similarities to that of toads, but also shows similarities with hylids and leptodactylids.

Taking into account similar morphological studies in bufonids (Jared et al., 2009, 2014; Mailho-Fontana et al., 2014a), leiopelmatids (Melzer et al., 2011), leptodactylids (Toledo and Jared, 1995; Lenzi-Mattos et al., 2005), and phyllomedusids (Antoniazzi et al., 2013), the present examination of *O. cultripes*, an odontophrynid species, contributes to the evidence that amphibians (at least anurans) share a basic design for all types of cutaneous glandular accumulations. This basic design seems to guide the formation of all macroglands along the evolutionary process. The determinant factor for macroglandular formation may be selective pressure for defense against specific predators of each group. However, this issue will be better elucidated as the natural history and toxin chemistry of the various species is studied more extensively.

Acknowledgments

We thank R. Kodama, H. Bonfim, R. Recoder, M. Teixeira Jr., and F. Dal Vechio for help in field, and ICMBIO (SISBIO #23202-1 and #10126-1, Ethics Committee on Animal Use of Instituto Butantan for permits and São Paulo Research Foundation (FAPESP #2014/15334-4 and #2015/00999-3) for financial support.

Appendix A. Supplementary data

Supplementary data related to this article can be found at http://dx.doi.org/10.1016/j.toxicon.2017.02.022.

Transparency document

Transparency document related to this article can be found online at http://dx.doi.org/10.1016/j.toxicon.2017.02.022.

References

Almeida, P.G., Felsemburgh, F.A., Azevedo, R.A., Brito-Gitirana, L., 2007. Morphological re-evaluation of parotoid glands of *Bufo ictericus* (Amphibia, Anura, Bufonidae). Contr. Zool. 73, 145–152.
Antoniazzi, M.M., Neves, P.R., Mailho-Fontana, P.L., Rodrigues, M.T., Jared, C., 2013. Morphology of the parotoid macroglands in *Phyllomedusa* leaf frogs. J. Zool. 291, 42–50.
Bancroft, J.B., Steven, A., 1990. Theory and Practice of Histological Techniques. Churchill Livingstone, Edinburgh.
Barthalmus, G.T., 1989. Neuroleptic modulation of oral dyskinesias induced in snakes by *Xenopus* skin mucus. Pharmacol. Biochem. Behav. 30, 957–959.
Borges-Nojosa, D.M., Carvalho Jr., R.R., Borges-Leite, M.J., Lima, D.C., Melo, J.C.L., Cascon, P., 2016. Defensive behaviors in two species of *Odontophrynus* Reinhardt and Lütken, 1862 (Anura: Odontophrynidae). Herpetol. Notes 9, 67–71.
Brodie Jr., E.D., Gibson, L.S., 1969. Defensive behavior and skin glands of the northwestern salamander, *Ambystoma gracile*. Herpetologica 25, 187–194.
Brodie Jr., E.D., 1983. Antipredator adaptations of salamanders: evolution and convergence among terrestrial species. In: Margaris, N.S., Arianoutsou-Faraggitaki, M., Reiter, R.J. (Eds.), Plant, Animal and Microbial Adaptations to Terrestrial Environment. Plenum, New York, pp. 109–133.
Brodie Jr., E.D., Smatresk, N.L., 1990. The antipredator arsenal of fire salamanders: spraying of secretions from highly pressurized dorsal skin glands. Herpetologica 46, 1–7.
Canelas, M.A.S., Bertoluci, J., 2007. Anurans from Serra do Caraça, southeastern Brazil species composition and phenological patterns of calling activity. Iheringia. Sér. Zool 97, 21–26.
Cannon, M.S., Palkuti, G.A., 1976. Parotoid gland of Bufonidae. Toxicon 14, 149–151.
Caramaschi, U., Napoli, M.F., 2012. Taxonomic revision of the *Odontophrynus cultripes* species group, with description of a new related species (Anura, Cycloramphidae). Zootaxa 3155, 1–20.
Chammas, S.M., Carneiro, S.M., Ferro, R.S., Antoniazzi, M.M., Jared, C., 2015. Development of integument and cutaneous glands in larval, juvenile and adult toads (*Rhinella granulosa*): a morphological and morphometric study. Act. Zool. 96, 460–477.
Clark, B.T., 1997. The natural history of amphibian skin secretions, their normal functioning and potential medical applications. Biol. Rev. 72, 365–379.
Daly, J.W., Spande, T.F., Garraffo, H.M., 2005. Alkaloids from amphibian skin: a tabulation of over eight-hundred compounds. J. Nat. Prod. 68, 1556–1575.
Delfino, G., Brizzi, R., Calloni, C.A., 1990. Morphofunctional characterization of the serous cutaneous glands in *Bombina orientalis* (Anura, Discoglosside). Zool. Anz 225, 295–310.
Delfino, G., Brizzi, R., Kracke-Bendorff, R., Alvarez, B., 1998. Serous gland dimorphism in the skin of *Melanophryniscus stelzneri* (Anura: Bufonidae). J. Morphol. 237, 19–32.
Duellman, W.E., Trueb, L., 1996. The Biology of Amphibians. MacGraw – Hill, New York.
Erspamer, V., Falconieri-Erspamer, G., Cei, J.M., 1986. Active peptides in the skins of two hundred and thirty American amphibian species. Comp. Biochem. Physiol. C 85, 125–137.
Felsemburgh, F.A., Carvalho-E-Silva, S.P., de Brito-Gitirana, L., 2007. Morphological characterization of the anuran integument of the *Proceratophrys* and *Odontophrynus* genera (Amphibia, Anuran, Leptodactylidae). Micron 38, 439–445.
Habermehl, G., 1981. Venomous Animals and Their Toxins. Springer, Verlag, Berlin.
Hödl, W., Amézquita, A., 2001. Visual signaling in anuran amphibians. In: Ryan, M.J. (Ed.), Anuran Communication. Smithsonian Inst. Press, Washington, pp. 121–141.
Hostetler, J.R., Cannon, M.S., 1974. The anatomy of the parotoid gland in Bufonidae with some histochemical findings. I *Bufo marinus*. J. Morphol. 142, 225–240.
Jared, C., Antoniazzi, M.M., Jordão, A.E.C., Silva, J.R.M.C., Greven, H., Rodrigues, M.T., 2009. Parotoid macroglands in toad (*Rhinella jimi*): their structure and functioning in passive defense. Toxicon 54, 197–207.
Jared, C., Mailho-Fontana, P.L., Antoniazzi, M.M., Mendes, V.A., Barbaro, K.C., Rodrigues, M.T., Brodie Jr., E.D., 2015. Venomous frogs use heads as weapons. Curr. Biol. 25, 2166–2170.
Jared, S.G.S., Jared, C., Egami, M.I., Mailho-Fontana, P.L., Rodrigues, M.T., Antoniazzi, M.M., 2014. Functional assessment of toad parotoid macroglands: a study based on poison replacement after mechanical compression. Toxicon 87, 92–103.
Junqueira, L.C.U., Bignolas, G., Brentani, R., 1979. Picrosirius staining plus polarization microscopy, a specific method for collagen detection in tissue sections. Histochem. J. 11, 447–455.
Junqueira, L.C.U., 1995. Histology revisited. Technical improvement promoted by the use of hydrophilic resin embedding. Ciênc. Cult 47, 92–95.
Laemmli, U.K., 1970. Cleavage of structural proteins during assembly of the head of bacteriophage T4. Nature 227, 680–685.
Lenzi-Mattos, R., Antoniazzi, M.M., Haddad, C.B., Tambourgi, D.V., Rodrigues, M.T., Jared, C., 2005. The inguinal macroglands of the frog *Physalaemus nattereri* (Leptodactylidae): structure, toxic secretion and relationship with deimatic behaviour. J. Zool. 266, 385–394.
Licht, L.E., Low, B., 1968. Cardiac response of snakes after ingestion of toad parotoid venom. Copeia 1968, 547–551.
Licht, L.E., Sever, D.M., 1993. Structure and development of the paratoid gland in metamorphosed and neotenic *Ambystoma gracile*. Copeia 1, 116–123.
Liu, Y., Xiao, Y., Xue, X., Zhang, X., Liang, X., 2010. Systematic screening and characterization of novel bufadienolides from toad skin using ultra-performance liquid chromatography/electrospray ionization quadrupole time-of-flight mass spectrometry. Rapid Commun. Mass Spectrom. 24, 667–678.
Lutz, B., 1966. Biological significance of cutaneous secretions in toads and frogs. Mem. Inst. Butantan 33, 55–59.
Lutz, B., 1971. Venomous toads and frogs. In: Bücherl, W., Buckey, E.E. (Eds.), Venomous Animals and Their Venoms. Academic Press, New York, pp. 423–473.
Maciel, N.M., Schwartz, C.A., Rodrigues Pires Júnior, O., Sebben, A., Castro, M.S., Sousa, M.V., Fontes, W., Ferroni Schwartz, E.N., 2003. Composition of indolealkylamines of *Bufo rubescens* cutaneous secretions compared to six other Brazilian bufonids with phylogenetic implications. Comp. Biochem. Physiol. B 134, 641–649.
Mailho-Fontana, P.L., 2012. Comparative Study of the Cutaneous Chemical Defensive System in Two Species of Amazonian Toads (*Rhinella marina* and *Rhaebo guttatus*). Dissertação (Mestrado em Toxinologia). Instituto Butantan, São Paulo, Brazil.
Mailho-Fontana, P.L., Antoniazzi, M.M., Toledo, L.F., Verdade, V.K., Sciani, J.M., Rodrigues, M.T., Jared, C., 2014a. Passive and active defence in toads: the parotoid macroglands in *Rhinella marina* and *Rhaebo guttatus*. J. Exp. Zool. 321, 65–77.
Mailho-Fontana, P.L., Cavalcanti, I.R.S., Abe, C.M., Antoniazzi, M.M., Jared, C., 2014b. Considerations about the Morphology and the Secretion of the Skin Glands of the "cururu" Toad *Rhinella jimi* (Reunião Científica Anual do Instituto Butantan).
McClean, S., Robinson, R.C., Shaw, C., Smyth, W.F., 2002. Characterization and determination of indole alkaloids in frog-skin secretions by electrospray ionization ion trap mass spectrometry. Rapid Commun. Mass Spectrom. 16, 346–354.
Melzer, S., Clerens, S., Bishop, P.J., 2011. Differential polymorphism in cutaneous glands of archaic *Leiopelma* species. J. Morphol. 272, 1116–1130.
Meyer, K., Linde, H., 1971. Collection of toads venoms and chemistry of the toad venom steroids. In: Bücherl, W., Buckley, E.E. (Eds.), Venomous Animals and Their Venoms. Academic Press, New York, pp. 521–556.
Pukala, T.L., Bertozzi, T., Donnellan, S.C., Browie, J.H., Surinyajohnson, K.H., Liu, Y., Jackway, R.J., Doyle, J.R., Lewellyn, L.E., Tyler, M.J., 2006. Host-defence peptide profiles of the skin secretions of interspecific hybrid tree frogs and their parents, female *Litoria splendida* and male *Litoria caerulea*. FEBS J. 273, 3511–3519.
Rash, L.D., Morales, R.A.V., Vink, S., Alewood, P.F., 2010. De novo sequencing of peptides from parotoid secretion of the cane toad, *Bufo marinus (Rhinella*

marina). Toxicon 57, 208–216.
Regueira, E., Dávila, C., Hermilda, G.N., 2016. Morphological changes in skin glands during development in *Rhinella arenarum* (Anura: Bufonidae). Anat. Rec. 299, 141–156.
Rollins-Smith, L.A., King, J.D., Nielsen, P.F., Sonnevend, A., Conlon, J.M., 2005. An antimicrobial peptide from the skin secretions of the mountain chicken frog *Leptodactylus fallax* (Anura:Leptodactylidae). Regul. Pept. 124, 173–178.
Sakate, M., Lucas De Oliveira, P.C., 2000. Toad envenoming in dogs: effects and treatment. J. Venom. Anim. Toxins 6, 1–9.
Savage, J.M., Cei, J.M., 1965. A review of the leptodactylid frog genus, *Odontophrynus*. Herpetologica 21, 178–195.
Sciani, J.M., Angeli, C.B., Antoniazzi, M.M., Jared, C., Pimenta, D.C., 2013. Differences and similarities among parotoid macrogland secretions in South American toads: a preliminary biochemical delineation. Sci. World J. 1–9.
Siano, A., Húmpola, M.V., de Oliveira, E., Albericio, F., Simonetta, A.C., Lajmanovich, R., Tonarelli, G.G., 2014. Antimicrobial peptides from skin secretions of *Hypsiboas pulchellus* (Anura: Hylidae). J. Nat. Prod. 77, 831–841.
Toledo, R.C., Jared, C., 1989. Estudo histológico das glândulas lombares de *Pleurodema thaul* (Amphibia, Anura, Leptodactylidae). Rev. Bras. Biol. 49, 421–428.
Toledo, R.C., Villa, N., 1987. Estudo histológico das glândulas tibiais de *Bufo paracnemis* (Amphibia, Anura, Bufonidae). Rev. Bras. Biol. 47, 204–215.
Toledo, R.C., Jared, C., 1995. Cutaneous granular glands and amphibian venoms. Comp. Biochem. Physiol. C 111, 1–29.
Tronchet, J., 1952. Contribution a l'étude histochimie des glandes parotoïdes du crapaud common *Bufo bufo* (Linné). Bull. Soc. Zool. Fr 77, 204–216.
Wilber, C.G., Carroll, P.L., 1940. Studies on the histology of the glands in the skin of Anura. The parotoid gland of *Bufo americanus holbrook*. Trans. Am. Microsc. Soc. 59, 123–128.
Ye, M., Guo, D.A., 2005. Analysis of bufadienolides in the Chinese drug ChanSu by high-performance liquid chromatography with atmospheric pressure chemical ionization tandem mass spectrometry. Rapid Commun. Mass Spectrom. 19, 1881–1892.